Article

NMR Dynamics of Transmembrane and Intracellular Domains of p75NTR in Lipid-Protein Nanodiscs

Konstantin S. Mineev,[1,*] Sergey A. Goncharuk,[1] Pavel K. Kuzmichev,[1] Marçal Vilar,[2] and Alexander S. Arseniev[1]
[1]Shemyakin-Ovchinnikov Institute of Bioorganic Chemistry, Moscow, Russian Federation; and [2]Neurodegeneration Unit, Unidad Funcional de Investigación de Enfermedades Crónicas-Instituto de Salud Carlos III, Madrid, Spain

ABSTRACT P75NTR is a type I integral membrane protein that plays a key role in neurotrophin signaling. However, structural data for the receptor in various functional states are sparse and controversial. In this work, we studied the spatial structure and mobility of the transmembrane and intracellular parts of p75NTR, incorporated into lipid-protein nanodiscs of various sizes and compositions, by solution NMR spectroscopy. Our data reveal a high level of flexibility and disorder in the juxtamembrane chopper domain of p75NTR, which results in the motions of the receptor death domain being uncoupled from the motions of the transmembrane helix. Moreover, none of the intracellular domains of p75NTR demonstrated a propensity to interact with the membrane or to self-associate under the experimental conditions. The obtained data are discussed in the context of the receptor activation mechanism.

INTRODUCTION

Neurotrophins (NTs) play a key role in the development and function of the nervous system. NTs exert their functions by binding to two different receptors: p75 NT receptor (p75NTR, a member of the tumor necrosis factor receptor (TNFR) family) and Trk receptor (a receptor tyrosine kinase). p75NTR binds to all mature and unprocessed NTs, such as nerve growth factor (NGF), brain-derived neurotrophic factor (BDNF), NT3, and NT4/5. Binding of NTs to p75 triggers different signaling pathways, including cell death, survival, neurodegeneration, and proliferation. The expression of p75NTR is downregulated in adults but can be enhanced upon neuronal insult or degeneration (1). This makes p75NTR a prospective target for the therapy of several diseases, including Alzheimer's disease (2–6), and an attractive object for structural investigations.

P75NTR has the architecture of a type I integral membrane protein, i.e., it has an extracellular ligand-binding domain (ECD), a single-span helical transmembrane domain (TMD), and an intracellular domain (ICD). The ICD of p75NTR can be divided into three parts: the chopper domain (residues 277–308) and linker region (309–338), which together form the juxtamembrane part of the ICD, and a death domain (DD) (7) (residues 339–417). The DD of p75NTR does not show any catalytic activity, and downstream signaling is thought to be launched by ligand-dependent recruitment of the cytoplasmic effectors to and from the domain (7,8). In addition to the DD, the chopper domain of p75NTR is also known to play a key role in p75NTR function. For instance, receptors with a deleted DD can trigger cell death if the chopper domain is still present (9). Moreover, a free chopper domain inhibits full-length p75NTR and protects neurons from cell death (9).

Vilar et al. (10) showed that p75NTR forms covalent dimers via the Cys-257 intermolecular disulfide bridge located in the TMD, regardless of ligand binding. Based on this finding, the authors proposed a so-called snail-tong mechanism for p75NTR activation (10), implying that both the ligand-bound and ligand-free receptor states are covalent dimers. According to the model, the ligand binding causes an interaction between the ECDs and release of the DDs, which are in a tight interaction in the inactive complex. This mechanism was further supported by the recent finding that free p75NTR ICDs are able to form homodimers at moderately high concentrations (11). On the other hand, the possibility of an intermolecular disulfide bond between the C379 residues of DDs was demonstrated by x-ray crystallography (12), which blurs our understanding of the p75NTR activation mechanism. Still, the described mechanism does not explain the role of the chopper domain in p75NTR activation, and the connection between the conformations of the TMDs and ECDs and the state of the intracellular part of the receptor is not yet understood. All available prediction software have indicated that the chopper and linker domains are intrinsically disordered (Fig. S1 in the Supporting Material) and the DD of p75NTR is connected to the TMD by a long and flexible linker (13). In this study, we investigated the spatial structure and dynamics of the juxtamembrane region and DD of p75NTR

Submitted April 28, 2015, and accepted for publication July 9, 2015.

*Correspondence: mineev@nmr.ru

Konstantin S. Mineev and Sergey A. Goncharuk contributed equally to this work.

Editor: Kalina Hristova.

0006-3495/15/08/0772/11

http://dx.doi.org/10.1016/j.bpj.2015.07.009

in the presence of its TMD in particles of different membrane mimetics.

MATERIALS AND METHODS

Gene construction and expression, and protein purification

Target genes encoding the p75-TMDCD fragment (residues 245–308), p75ICD fragment (residues 288–425), or p75-ΔECD fragment (residues 245–425) of rat wild-type p75 were cloned into the pGEMEX-1 vector with a polyhistidine tag and thrombin cleavage site. Genes were expressed either by a continuous-exchange cell-free (CF) system with the addition of isotope-labeled amino acids (14,15) (p75ICD and P75TMDCD) or in a bacterial culture of the *E. coli* BL21(DE3) strain (p75-ΔECD) in minimal salt media. CF extract from the BL21(DE3) *E. coli* strain and T7 RNA polymerase were prepared according to a previously described protocol (16). To obtain ^{15}N-labeled or ^{15}N-^{13}C-labeled proteins, we used $^{15}NH_4Cl$ or $^{15}NH_4Cl$ and ^{13}C-glucose, respectively. Target proteins were purified on a Ni Sepharose HP column and 6-histidine tags were cleaved by thrombin. p75-TMDCD was purified by size-exclusion chromatography in lauryl sarcosine micelles and precipitated according to the trichloroacetic acid/acetone procedure (17).

To prepare lipid-protein nanodiscs (LPNs), we used plasmid vectors with the membrane scaffold proteins (MSPs) MSP1, MSP1D1ΔH5, and MSP1D1ΔH4H5H6 (kindly provided by E. Lyukmanova and G. Wagner). We achieved high-level expression of all MSP variants by using the BL21(DE3) strain and autoinduction system with ZYM-5052 medium (18). For purification of all MSPs, we used the protocol described by Ritchie et al. (19) with some modifications.

Sample preparation and assembly of LPNs

p75-TMDCD was dissolved by the addition of dodecylphosphocholine (DPC) micelles or a DMPC dimyristoylphosphatidylcholine (DMPC)/dihexanoylphosphatidylcholine (DHPC) 1:3 bicelle solution (pH 6.0, 20 mM NaPi, 40°C). The lipid/protein ratio (LPR) was maintained at 35–40:1 to ensure protein dimerization. To assemble the LPNs, the lipid mixture, 3-[(3-cholamidopropyl)-dimethylammonio]-1-propanesulfonate (CHAPS), and MSPs were added to the sample in DPC micelles. Then, Bio-Beads SM-2 resin (Bio-Rad; 1 g per 70 mg of detergent) was added and the suspension was shaken at room temperature for 24 h. The Bio-Beads resin was removed by centrifugation and the supernatant was concentrated to obtain an NMR sample.

To obtain p75-ΔECD in a micellar environment, we removed lauryl sarcosine by several cycles of dilution with DPC buffer (20 mM Tris pH 8.0, 100 mM NaCl, 1 mM dithiothreitol (DTT), 0.5% DPC) and concentration on 30 kDa centrifugal filter units.

To prepare an LPN-p75-ΔECD solution, we first suspended the desired lipid or lipid mix in ND buffer (20 mM Tris pH 8.0, 100 mM NaCl, and 10 mM DTT) with CHAPS (1:1 lipid/CHAPS). If not otherwise stated, a 4:1 DMPC/dimyristoylphosphatidylglycerol (DMPG) mixture was used for the LPN preparation. The desired MSP variant and p75-ΔECD in lauryl sarcosine were added to the lipid solution and incubated for 1 h. The LPR was varied in the range of 130:1 to 10:1 to obtain one or several p75-ΔECD proteins per LPN. Bio-Beads SM-2 resin (1 g per 70 mg of detergent) was added and the suspension was shaken at room temperature for 12–16 h. The Bio-Beads resin was removed by centrifugation and washed twice with ND buffer. To remove LPNs without target protein, we performed metal affinity chromatography using Ni Sepharose HP resin. LPNs with p75-ΔECD were eluted in ND buffer with 500 mM of imidazole. The protein sample was concentrated and the buffer was changed to NMR buffer (20 mM NaPi, pH 6.7, 50 mM NaCl, 5 mM DTT, and 0.01% NaN3) by several cycles of dilution and concentration with 30 kDa centrifugal filter units.

NMR spectroscopy

All NMR spectra were acquired on Avance III 600 and 800 MHz spectrometers (Bruker BioSpin, Germany) equipped with cryogenic triple-resonance probes, at pH 6.5–7.2 and 30°C. Assignment of chemical shifts was performed according to the standard approach (20) with the use of triple-resonance and NOESY 3D NMR spectra. Nonuniform sampling in indirect dimensions (21) and BEST-TROSY (22) pulse sequences were used to detect the triple-resonance spectra. Pseudo-3D HSQC-based pulse sequences were used to measure the NMR relaxation parameters (23). Cross-correlated relaxation rates were determined as described previously (24). The size of the LPNs was determined from the translational diffusion coefficients, measured by NMR with the use of stimulated-echo and bipolar gradients (25). TALOS+ software was used to predict the secondary structure and mobility of the protein based on NMR chemical shifts (26).

More details regarding the experimental protocols used in this work can be found in the Supporting Materials and Methods.

Database entries

The assigned chemical shifts of the p75-TMDCD construct in DPC micelles and MSP1 LPNs, and of the p75-ΔECD protein in MSP1 LPNs were deposited in the BMRB database (http://www.bmrb.wisc.edu) under accession codes 25647, 25648, and 25646, respectively.

RESULTS

The chopper domain of p75NTR is unstructured in the presence of TMD in a variety of membrane mimetics

To study the structural properties of the p75NTR chopper domain, we first prepared a construct containing the TMD and chopper domain of rat p75 (p75-TMDCD, residues 245–308, UniProt ID: P07174) and incorporated it into particles of a membrane mimetic (DPC micelles, 1:3 DMPC/DHPC bicelles and DMPC/DMPG 4:1 LPNs assembled using MSP1 at pH 6.5 and 50 mM NaCl). This construct was previously shown to cause cell death in neurons (9,27), and therefore we can expect that the conformation of the chopper domain is close to physiologically relevant. All three types of membrane mimetics allowed the acquisition of high-resolution NMR spectra and chemical shift assignment, which was performed for the DPC and LPN samples (Fig. S2). Signals from the transmembrane part of the protein were observed only in micellar and bicellar environments, and the chopper signals were narrow and intense in the spectra acquired for all samples. As there is no criterion for judging the nativity of various membrane mimetics for p75-TMDCD, we a priori assumed that the LPNs provide the most native environment (28); however, we tried to characterize the structural and dynamic properties of the chopper domain in both micelles/bicelles and nanodiscs.

To obtain information about the structure and dynamics of p75-TMDCD, we used the chemical shift index (CSI) as an indicator of secondary structure and the ^{1}H-^{15}N cross-correlated relaxation rate (η_{xy}) as an indicator of disorder and backbone mobility. According to the NMR chemical shift data, the transmembrane helix ranged from

L253 to W276, and the chopper domain (N277–I308) was disordered (Fig. 1 *A*). Surprisingly, whereas the (^{1}H,^{15}N) chemical shifts of the transmembrane residues differed substantially for the micelle and bicelle solutions, the chopper signals remained unchanged in all three tested membrane mimetics, suggesting that the chopper domain does not interact with the membrane (Figs. 1 *C* and S4). This is further supported by the NMR relaxation data. The η_{xy} magnitudes did not differ from zero within the experimental error for the vast majority of chopper residues (except for the N277-Q281 in micelles and N277-K283 in nanodiscs, which are located in proximity to the surface of the membrane-mimetic particle) in both micelles and nanodiscs, indicating that the chopper domain is disordered and very flexible, with motions on a subnanosecond timescale (Fig. 1 *B*). Moreover, we need to note here that the reported data were obtained in micelles at an LPR of 35, when the major part of the protein was forming a dimer via the C257 disulfide bond, and at LPR = 140, when mostly the entire protein was monomeric (Figs. S4 and S5). Formation of the transmembrane disulfide bond was determined by reducing and nonreducing SDS-PAGE (Fig. S2). Dilution by detergent in the presence of 5 mM of DTT did not change the behavior of the chopper domain, whereas the chemical shifts of the TMD changed and the dimer-monomer transition occurred (Fig. S5). Therefore, the chopper domain is disordered regardless of the dimeric or monomeric state of p75-TMDCD in a DPC environment. In the case of LPNs and bicelles, Cys-257 disulfide was not formed, due to the high LPR. To summarize, we have shown here that the chopper domain of p75NTR is unstructured, highly flexible, and mobile, and does not interact with membrane mimetics.

Screening for optimal conditions to study p75 with deleted ECD

To study the structure of the chopper domain in a more native environment and investigate the dynamic behavior of the intracellular part of p75NTR in the presence of the membrane, we produced a 21 kDa protein corresponding to the receptor with deleted ECD (p75-ΔECD, residues 245–425, UniProt ID: P07174, with an additional N-terminal polyhistidine tag and thrombin recognition site). Since p75-ΔECD is a multidomain protein that can be unfolded by a detergent (29), a thorough screening procedure is necessary to find the optimal membrane mimetic. For this purpose, we incorporated p75-ΔECD at an LPR of 120–130 into DPC micelles, DMPC/DHPC bicelles, DMPC/CHAPS bicelles, and LPNs containing a DMPC/DMPG 4:1 mixture, and compared 2D ^{1}H,^{15}N-TROSY NMR spectra of p75-ΔECD with the spectra of p75NTR ICD (p75ICD, residues 288–425) obtained in aqueous buffer with the same composition and pH (Figs. 2 *A* and S6). Experiments were run in the presence of DTT, and no intermolecular disulfide bonds were formed. The results revealed that only the LPNs retained the characteristic spectrum of the DD, and the detergent of micelles and bicelles caused unfolding of the domain. DMPC/CHAPS bicelles also

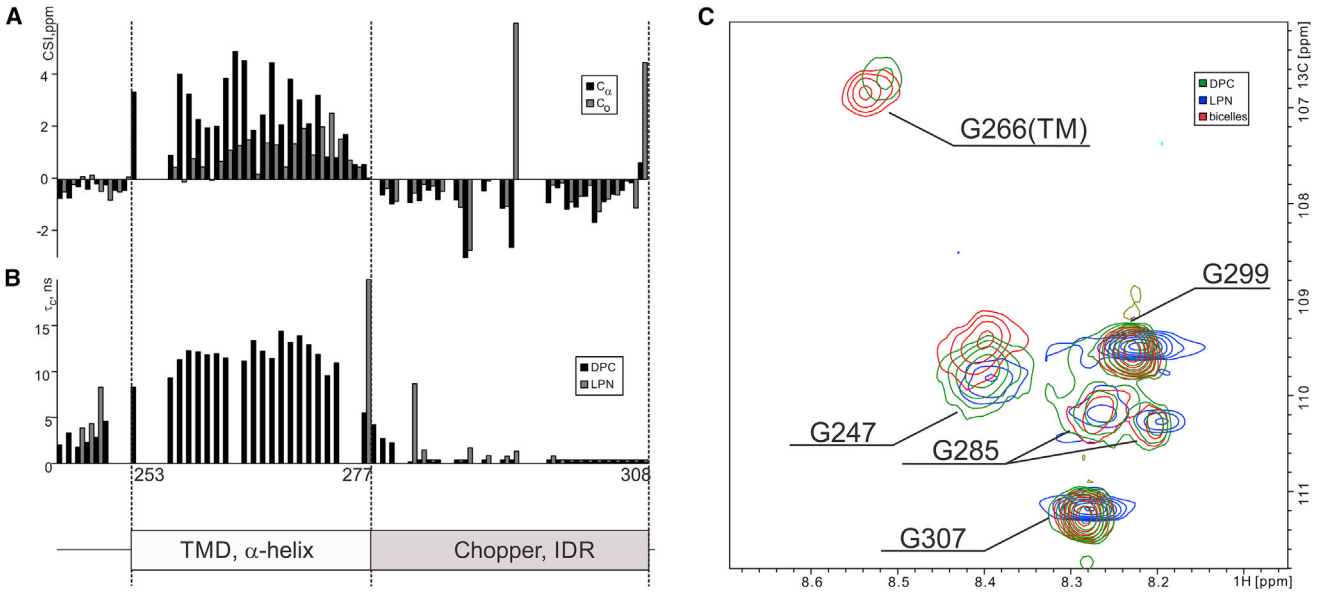

FIGURE 1 Structure and dynamics of the chopper domain in the context of the p75-TMDCD construct. (*A*) ^{13}Cα and ^{13}Co secondary chemical shifts of p75-TMDCD in DPC micelles (chemical shifts of chopper in LPNs do not differ within the experimental error). (*B*) Rotational correlation time (τ_C) of N-H groups determined from the cross-correlated ^{1}H-^{15}N relaxation rate in DPC micelles (*black bars*) and LPNs (*gray bars*). (*C*) Overlay of the glycine region of the ^{1}H,^{15}N-HSQC spectra of p75-TMDCD acquired in DPC micelles (*green*), DMPC/DHPC 1:3 bicelles (*red*), and DMPC/DMPG 4:1 MSP1 LPNs. All spectra were acquired at pH 6.5, 20 mM NaPi, and 30°C. LRP was equal to 35 in micelles, 200 in bicelles, and 130 in LPNs. To see this figure in color, go online.

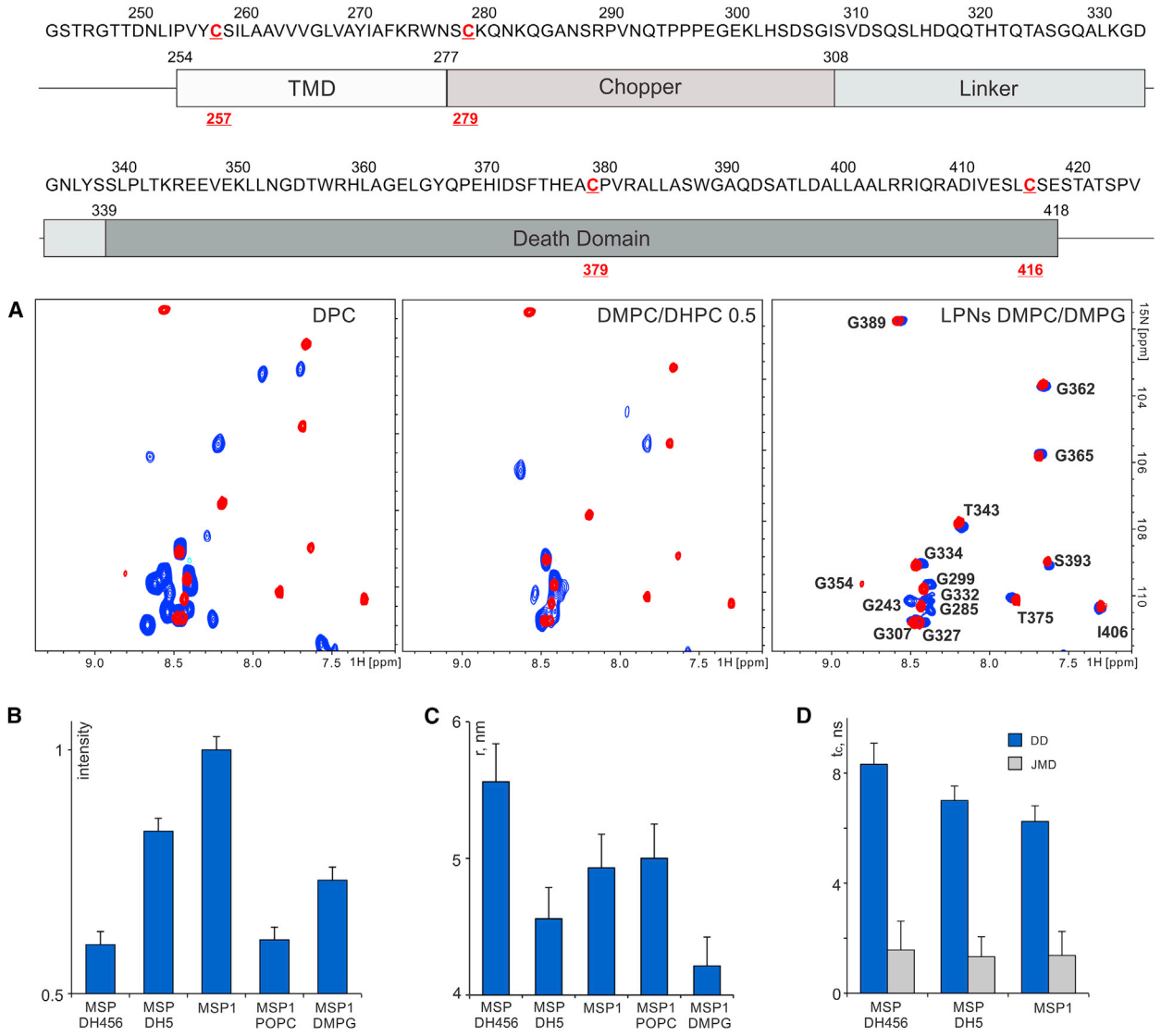

FIGURE 2 Screening of membrane mimetics for structural studies of p75-ΔECD. (*A*) Glycine region of the ^{1}H,^{15}N-HSQC spectrum of p75-ΔECD acquired in DPC micelles, DMPC/DHPC $q = 2{:}5$ bicelles, and DMPC/DMPG MSP1 LPNs (*blue peaks*) at LPR = 130. The spectrum of p75ICD (the DD is folded), acquired in aqueous solution at the same temperature, pH, and ionic strength, is shown in red. (*B–D*) Relative intensity of the signals from the DD of p75-ΔECD in ^{1}H,^{15}N-HSQC spectra, hydrodynamic radii of LPNs with incorporated p75-ΔECD, and average correlation time of rotational diffusion (τ_C) of the DD (*blue bars*) and juxtamembrane domain (JMD, includes the chopper and linker residues) (*gray bars*) of p75-ΔECD measured in LPNs formed by different variants of MSP and with various lipid contents (DMPC, POPC, and DMPG). The τ_C magnitudes were measured from the cross-correlated ^{1}H-^{15}N relaxation rates (24). The amino acid sequence of p75-ΔECD (excluding the expression tags) is shown together with the tertiary structure of p75NTR in the top panel. To see this figure in color, go online.

provided a fraction of the folded DD, but at a high lipid/detergent ratio (at least 1:1) and low concentration of p75-ΔECD (50 μM). Only signals from the extramembrane parts of p75-ΔECD were observed in the LPN sample, where discs were formed by the full-length MSP (MSP1) (30), even for the perdeuterated p75-ΔECD. We decided to continue the search for better conditions by testing the LPNs containing lipids with unsaturated acyl chains (POPC), LPNs assembled of anionic lipids (DMPG) only, and LPNs made using shortened variants of MSP as described by Hagn et al. (31).

These shortened MSPs were shown to provide smaller LPNs, which may allow the detection of signals from the TMD of p75-ΔECD. We compared three MSP variants: the full-length MSP1 (the theoretical mass of the LPN particle is equal to 124 kDa), MSP1D1ΔH5 (95 kDa), and MSP1D1ΔH4H5H6 (52 kDa). The LPNs were assembled with an excess of lipid to ensure a 1:1 protein per LPN distribution. None of the tested LPNs allowed the detection of signals from the p75NTR TMD, but, surprisingly, an inverse correlation was found between the size of the MSP and the intensity of the DD signals, and the intensities of the

chopper and linker signals were almost the same for all five samples (Fig. 2 *B*). POPC and DMPG in LPNs appeared to reduce the intensity of the DD crosspeaks in NMR spectra of p75-ΔECD.

In an attempt to understand the behavior of the protein in LPNs, we measured the translational diffusion of the LPNs by NMR (Fig. 2 *C*) and assessed the rotational diffusion of the p75NTR DD, chopper, and linker regions based on the cross-correlated relaxation rates (Fig. 2 *D*). We observed no direct correlation between the size of the nanodisc and the coefficient of translational diffusion, suggesting that the mobility of LPNs with p75-ΔECD is governed by the compactness of the ICD. This was as expected, because the size of the p75 ICD exceeds the diameter of the nanodisc and may reach 20 nm if the whole juxtamembrane region is in the extended conformation. Such compactness is maximal in the case of the DMPG MSP1 LPNs, which diffuse almost as fast as the empty LPNs (~4 nm), and is minimal for the MSPD1ΔH4H5H6 particles with a hydrodynamic radius close to 5.5 nm. One can easily see that the p75 ICD is more compact in larger LPNs, suggesting that it is capable of engaging in transient and short-lived interactions with the membrane, preferably with anionic headgroups. At the same time, the mobility of the receptor DD increases gradually with the size of the LPN (Fig. 2 *D*), whereas the mobility of the juxtamembrane regions is unchanged and extremely high. This is possible if the DD can occasionally interact with the MSP. In larger discs, the probability of such an interaction is decreased, resulting in increased mobility of the domain. To sum up, we have shown that LPNs composed of MSP1 and a mixture of anionic and zwitterionic lipids provide the best conditions for studying the structure and dynamics of the p75NTR ICD by NMR.

Structure and dynamics of p75-ΔECD in LPNs

To obtain a full set of data regarding the structure and intramolecular mobility of p75-ΔECD, we incorporated ^{15}N- and ^{13}C/^{15}N-labeled variants of the protein into MSP1 nanodiscs under reducing conditions (5 mM of DTT) and at an LPR of 130 (approximately one protein per nanodisc) for chemical shift assignment and NMR relaxation analysis. Crosspeaks in the ^{1}H,^{15}N-TROSY spectrum of p75-ΔECD can be easily divided into two subsets corresponding to the DD and flexible linker between the TMD and DD, including the chopper. Signals of the DD in p75-ΔECD exactly coincide with the spectrum of the isolated DD in PBS (Figs. 2 *A*, S6, and S7), suggesting that the spatial structure of the domain is not affected by the LPN membrane. Moreover, the chemical shifts are very similar to those reported by Liepinsh et al. (13), and thus the spatial structure of the DD is identical to PDB ID: 1NGR, which is supported by the chemical-shift-based secondary structure prediction (Fig. 3). On the other hand, the whole linker region of the protein that can be observed in LPNs (residues 284–338), including the major portion of the chopper domain and an additional 30 amino acid residues, is disordered. In addition, the signals of the chopper domain (residues 284–303) are located in almost the same positions as observed for p75-TMDCD in micelles, bicelles, and LPNs, implying that the conformational space of the chopper residues is not restricted by the presence of the DD. The signals of residues 304–308 of p75-TMDCD are shifted in comparison with the ΔECD construct, most likely due to the charge at the C-terminus of the shorter protein.

To study the motions of p75-ΔECD in MSP1 LPNs, we measured the ^{15}N NMR relaxation parameters for the vast majority of the protein residues, which gave rise to detectable signals in ^{1}H,^{15}N-HSQC. We determined the longitudinal (T_1) and transverse (T_2) relaxation times, heteronuclear ^{1}H-^{15}N NOE (NOE), and cross-correlated relaxation rates (η_{xy}), which allowed a straightforward interpretation. As expected, the NMR relaxation data (Fig. 3) reveal an extremely high mobility of the linker-chopper region (on average 2 ns rotational correlation time, negative NOE, ~0.4 s T_2, and ~2 s^{-1} η_{xy}) and the DD of p75-ΔECD (6.3 ± 1 ns, NOE ~0.9; Figs. 2 and 3). The mobility of the DD in the context of p75-ΔECD is equal within the experimental error to that observed for the isolated domain at the same temperature (6.5 ± 1 ns). Therefore, we can conclude that the motions of the DD are completely uncoupled from the TM helix and LPN, and the domain is folded and relatively stable. The linker region and chopper domain perform motions on a picosecond timescale and are completely disordered and flexible. Neither of these domains demonstrates any pronounced propensity for stable membrane binding.

Interaction between the DDs of p75-ΔECD

To explore the possibility of an interaction between the DDs of p75NTR, we assembled MSP1 nanodiscs with p75-ΔECD at various LPRs (130 (one protein per disc), 90 (~3:2), 60 (~2:1), and 20 (~6:1); Figs. S3 and S8). We failed to assemble LPNs with C257 disulfide dimer. The protein chain contains four cysteines, and they start to form multiple disulfide bridges under oxidizing conditions, which results in oligomerization of the protein. Therefore, all experiments were performed under highly reducing conditions (which are present in the cytosol in nonstressed situations). This experiment was designed to induce the close proximity of several p75NTR entities and trigger dimerization of the DDs, if possible. The initial characterization of the samples revealed a simple pattern: the intensity of the signals from DD residues, the compactness of the p75NTR ICD, and the mobility of the DD decreased with an increase of the average protein contents per LPN particle (Fig. 4, *A–C*). These effects were more pronounced in the case of smaller LPNs (Fig. 4 *C*). On the other hand, no chemical-shift changes were observed, suggesting that the structure of

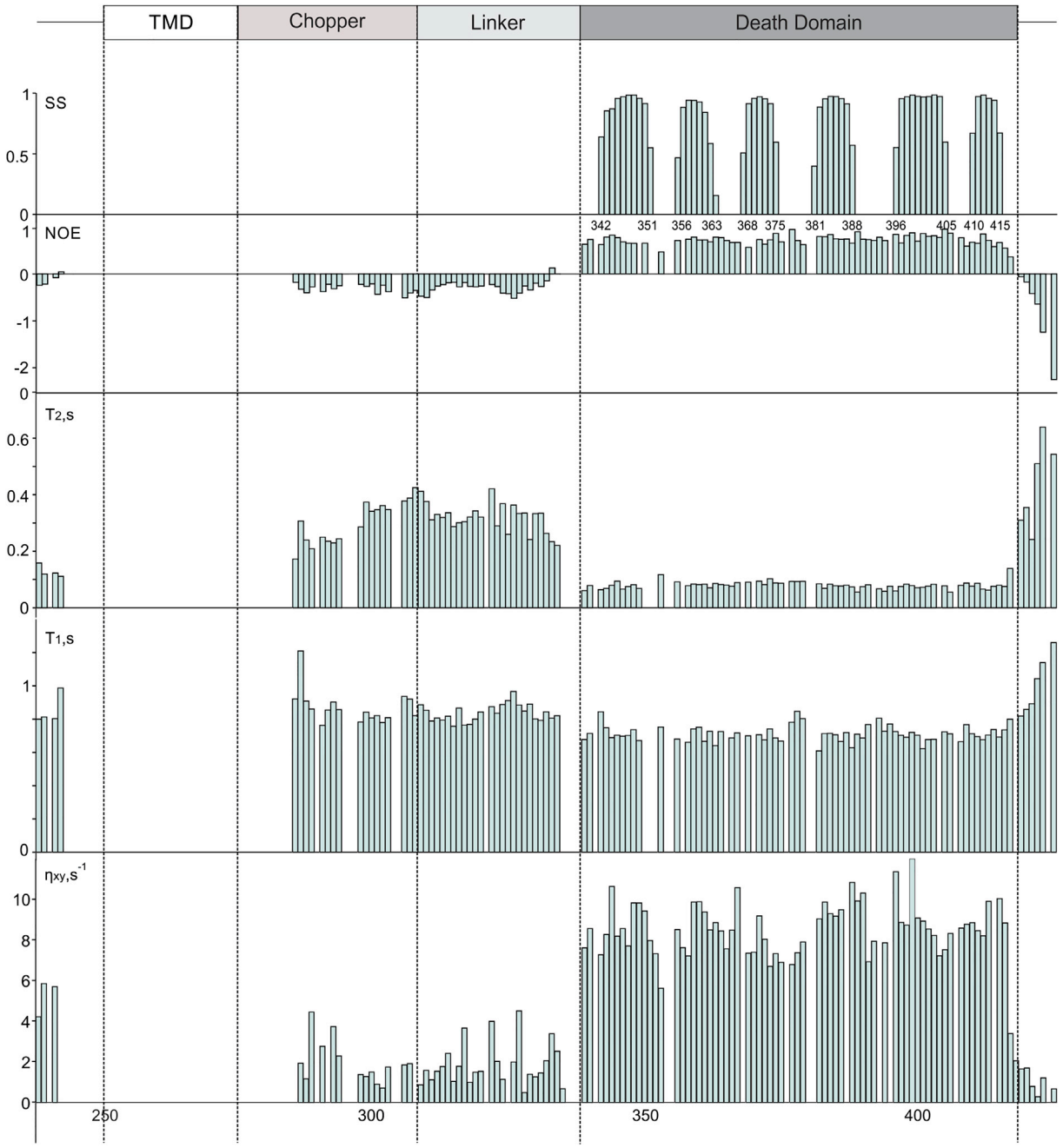

FIGURE 3 Secondary structure and mobility of p75-ΔECD in LPNs formed by MSP1. NMR relaxation parameters: longitudinal (T_1) and transverse (T_2) relaxation times, rates of cross-correlated ^{1}H-^{15}N relaxation (η_{xy}), magnitudes of heteronuclear ^{1}H-^{15}N NOE (NOE), and α-helix propensity (SS) are plotted versus the residue number in the amino acid sequence of p75NTR. SS was calculated using TALOS+ software (26) based on the ^{13}C chemical shifts. NMR parameters were measured at pH 6.8, 30°C, and 70 mM salt concentration. The transmembrane and five to 10 adjacent residues were not observed. To see this figure in color, go online.

the DD, the conformational space of the chopper and linker residues, and the environment of the DD amide groups remained unchanged in the whole sampled range of nanodisc populations. Moreover, the rotational diffusion of the DD changed just slightly (it increased by ~1.5 ns in 6:1 MSP1 discs compared with 1:1 MPS1 discs), and was still much faster than expected for a dimer of isolated DDs. Certainly, it is possible that there exists a stable dimeric state that was not observed in the NMR spectra due to line broadening beyond detection. However, according to our data, whereas the relative (per unit of the protein concentration) intensity of the DD signals was decreased at a high protein/LPN ratio, the intensity of the chopper and linker signals was almost unchanged. Therefore, even if the invisible dimer state

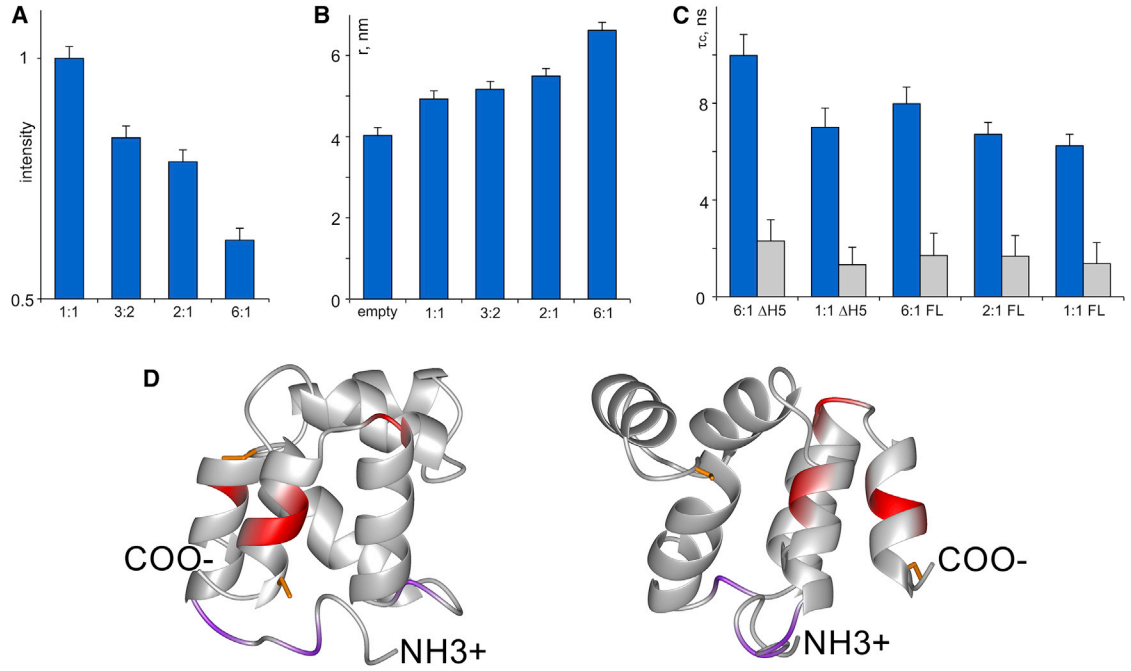

FIGURE 4 (*A*) Relative intensity of the signals from the DD of p75-ΔECD in $^{1}H,^{15}N$-HSQC spectra, acquired in MSP1 LPNs formed at various LPRs (number of p75-ΔECD copies per LPN). (*B*) Hydrodynamic radii of MSP1 LPNs with incorporated p75-ΔECD, formed at various LPRs, as determined from the NMR-derived translational diffusion coefficients. (*C*) Mean correlation time of rotational diffusion (τ_C) of the DD (*blue bars*) and chopper and linker residues (*gray bars*) of p75-ΔECD, measured in MSP1(FL) and MSP1D1ΔH5 (ΔH5) LPNs and formed at various LPRs. (*D*) Residues with accelerated transverse relaxation, taking part in slow transitions, are indicated in purple (N-terminal site) and red (C-terminal site) on the spatial structure of the DD of p75NTR (13) (PDB ID: 1NGR). To see this figure in color, go online.

exists, it is not characterized by stabilization of the flexible juxtamembrane regions. Additionally, the decrease in the intensity of the DD signals with the increase of the protein/LPN contents was gradual and could be explained by the altered relaxation parameters of the observed monomeric state. Besides, in the 6:1 LPNs, at least three proteins are in a parallel orientation, and their mobility would be restricted by the size of the LPN, which does not exceed 10–12 nm. Such conditions correspond to a relatively high effective concentration (>1 mM) of the DD. Therefore, we can state that the colocalization of several copies of p75-ΔECD in the same LPN does not induce a stable and specific association of the receptor DDs under reducing conditions, and only transient and nonspecific interactions are observed.

This conclusion was further supported by a more thorough analysis that included the measurement of ^{15}N NMR relaxation parameters for p75-ΔECD in 6:1 MSP1 LPNs (Fig. S9). We observed uniform changes in T_1, characterizing the mobility of the p75-ΔECD DDs, whereas the longitudinal relaxation times of the chopper and linker residues were almost unchanged. At the same time, changes in transverse relaxation, which includes contributions from slow motions and/or conformational rearrangements on a microsecond–millisecond timescale, were not that uniform. Seven residues demonstrate much faster transverse relaxation in the populated LPNs (6 p75-ΔECD copies per nanodisc). These residues take part in slow motions, according to the T_2 versus η_{xy} analysis (Fig. S9), and can be divided into two surfaces based on their location: S339, L342, and A394 form the first site at the N-terminus of the domain (*purple* in Fig. 4 *D*), and E412, V413, I406, and E349 form the second site (*red* in Fig. 4 *D*). These two sites may represent the interfaces for either the transient and unstable interaction of the receptor DDs or the interaction between the DD and MSP of the nanodisc. Such interactions do not induce detectable changes in the environment of the amide groups of the domain, but may cause a slight deceleration of its rotational diffusion.

DISCUSSION

Nanodiscs as a versatile medium for structural and functional studies of type I integral membrane proteins

Type I integral membrane proteins, which possess only a single transmembrane helix and large extra- and intracellular water-exposed domains, are extremely important for cell biology because they regulate a number of essential processes in living cells. Type I proteins include receptor tyrosine kinases, transforming growth factor receptor, toll-like receptors, and the TNFR family (including p75NTR), all of which are prospective targets for emerging therapies.

At the same time, these proteins are very difficult objects for structural studies. They have not yet been crystallized in a full-length form, and are usually too large for solution NMR spectroscopy. In addition, they require a very thorough search for a membrane mimetic to accommodate the transmembrane helix and to retain the native state of large extramembrane domains. Recent studies have demonstrated that detergent micelles, which are widely used in solution NMR spectroscopy of membrane proteins, sometimes have little applicability for proteins with large water-soluble domains, due to the ability of the detergent to unfold the extramembrane domains (29). As we show here, the detergent present in bicelles is also able to cause unfolding or wrong folding of the soluble globular domains of type I membrane proteins. Bicelles of a certain composition (DMPC/CHAPS, in this study) can be used, but their applicability is limited to a very narrow and uncomfortable range of protein and lipid concentrations. This presents a nice prospect for the use of LPNs as a membrane mimetic for structural studies of multidomain membrane proteins, especially since LPNs have been shown to be a perfect medium for the refolding of membrane proteins (32). Nanodiscs were first proposed as a reference medium for detergent screening (28) or as a possible environment in which to study the topology of small peptides in the membrane (33–36); however, recent advances, such as the development of new MSPs that form smaller discoid particles (up to ~50 kDa) (31), isotope labeling strategies, and NMR experimental techniques have also made them applicable for structural studies of membrane proteins (37). In this work, we show that a transmembrane protein with a relatively large water-soluble domain (p75-ΔECD) can be incorporated into LPNs of various sizes and studied by the conventional means of solution NMR spectroscopy to obtain biologically relevant structural data. In addition, we studied the impact of several types of MSPs on the size of LPNs and the quality of NMR spectra, and revealed that when a soluble domain has a propensity to bind MSPs, larger LPNs may yield better spectra.

Taking into account the above observations, we propose a strategy for conducting structural studies of type I membrane proteins or other membrane proteins with large soluble globular domains. The structural data concerning these proteins is fragmentary: x-ray or NMR structures of the isolated domains are available, but the correspondence between the possible conformations of different domains is poorly understood. To address this issue, we suggest that the structure and dynamics of constructs containing the transmembrane and one of the extramembrane globular domains of a membrane protein in an LPN environment (or both the ECD and ICD) should be investigated. Such studies could achieve several objectives: 1) establish a connection between the conformation of the transmembrane and the soluble domain of the protein; 2) determine the conformation of the soluble domain in almost native environment, including the TMD and a patch of a lipid bilayer; and 3) determine the binding sites or intermolecular interfaces for various effector molecules or drugs on the surface of the soluble domain under native-like conditions. To be fair, we did not manage to observe all transmembrane and five to 10 of the juxtamembrane residues in LPNs, so additional experiments on shorter constructs in other membrane mimetics are necessary to study the behavior of the TMDs themselves. Nevertheless, we presume that such information on the TMD can be obtained from samples with selectively protonated methyl groups (38) or segmental isotope labeling (39).

Behavior of p75-ΔECD in the context of receptor activation

To illustrate the practical significance of the structural data obtained in LPNs for multidomain membrane proteins, we analyzed the structural and dynamic information on the p75-ΔECD and p75-TMDCD obtained in LPN solution with regard to the p75NTR activation mechanism in the case of NGF/NT-mediated signaling. We found that 1) ICDs of p75NTR did not oligomerize or dimerize when several copies of the receptor with the deleted ECD occupied the same LPN; 2) the motions of the DD were uncoupled from the TMD helix; 3) the structures of both the chopper-linker region and the DD of p75NTR did not depend on the presence of the other domains and lipid bilayer models used here; 4) the chopper domain and linker region were disordered in all tested contexts and environments; and 5) none of the p75NTR ICDs revealed a propensity to interact with the model membrane, and only very transient interactions with anionic lipids were detected. Altogether, these data provide insight into the mechanism of receptor activation.

Recent functional studies of p75NTR signaling revealed the key role of the C257 intermolecular disulfide bond in receptor activity (10). The receptor can form covalent dimers in the absence of the ligand (10), and a ligand-independent receptor activation can be caused by the Cys cross-linking in the N-terminal juxtamembrane region, which could emulate ligand binding (40). Some effector proteins (such as TRAF-6 and NRIF) only interact with disulfide dimers (10), and the C257A mutant is unable to signal like wild-type p75 via different pathways. These findings point to a snail-tong mechanism of activation (Fig. 5 *A*) involving a ligand-mediated rearrangement of the covalent TMD dimer that in turn breaks the interaction between the DDs, which is assumed to be possible only in the inactive state. Finally, the monomerized DDs are now able to recruit the effector molecules and launch the downstream cascade. This process is realistic only if the conformation or the interaction of the p75NTR DDs is sensitive to the conformation of its TMD, which is difficult to imagine based on the data reported here. Any information on the TMD conformation seems to

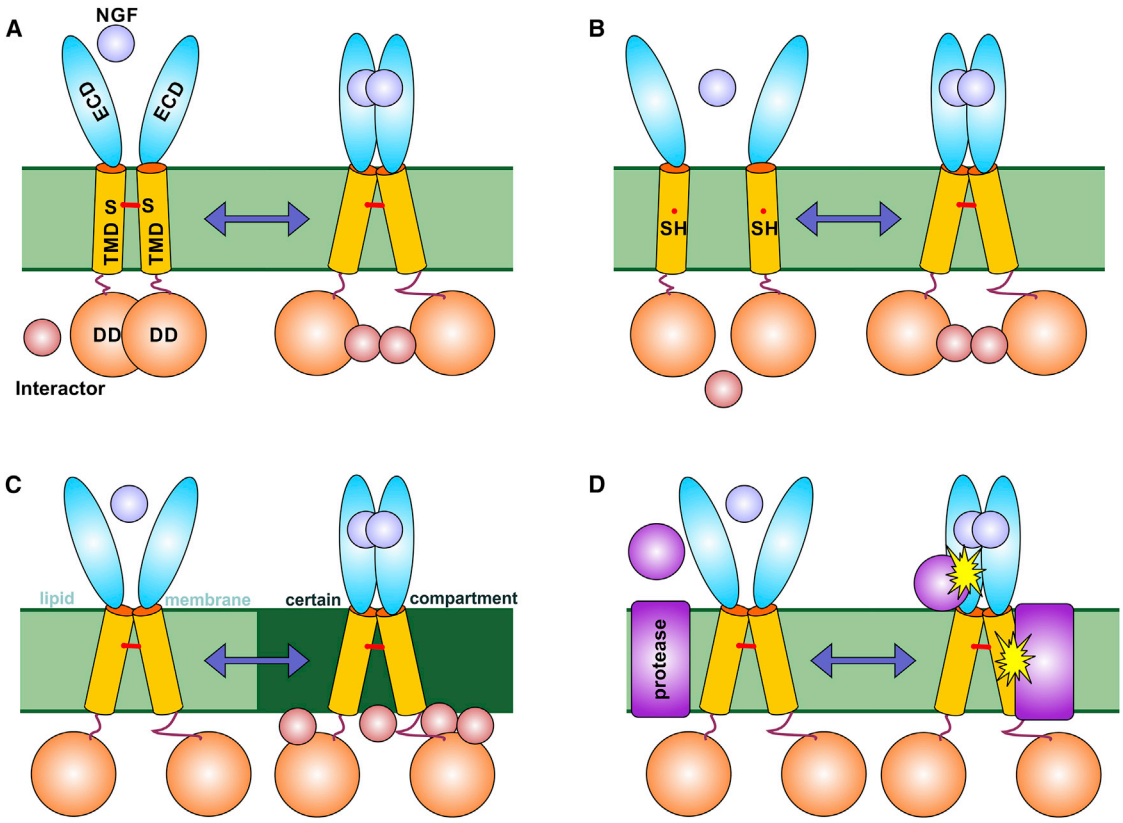

FIGURE 5 Possible mechanisms of p75NTR activation. (*A*) Snail-tong model. (*B*) Ligand-induced dimerization. (*C*) Migration to a certain compartment upon ligand binding. (*D*) Proteolytic processing upon ligand binding. To see this figure in color, go online.

be lost in a flexible and highly mobile linker connecting the DD to the membrane.

A number of studies have shown that the chopper domain of p75NTR is both necessary and sufficient for cell death signaling (9,27), and, moreover, the chopper region binds certain effector molecules, such as TRAF-6 (41), NADE (42), NRIF (43), and others (44). In this respect, the chopper domain will also have to feel the difference between the ligand-bound and free forms of the p75NTR TMD if the receptor is a covalent dimer (via the C257 disulfide bond) in both the active and inactive states. This is unlikely, because, as shown in this work, the chopper and linker domains are highly flexible and disordered. However, we have to admit that the chopper domain, being an intrinsically disordered region, may act via several processes that are not necessarily related to p75/NGF signaling, or the reported activity of the free chopper could be an effect of the sequestering of intracellular interactors with different outputs.

Another problem with respect to the p75NTR activation mechanism is the possibility of p75NTR DD dimerization. A number of studies have been dedicated to this problem, but the reported results are extremely controversial. Some works state that the DDs of p75NTR do not interact in solution (13), whereas a recent study showed that DDs are able to form weak dimers in specific conditions (11). Another work proposed that DDs can dimerize via the disulfide bridge between C379, which seems to be confirmed by mutagenesis (12) but contradicts the dimerization assays performed by other groups (10). Here, we found that the DDs did not demonstrate any dimerization propensity if several copies of the p75-ΔECD were in close proximity in the same nanodisc under reducing conditions, even at relatively low (1 mM) concentrations of the reducing agent (DTT). The experimental conditions seemed rather physiological, i.e., we worked at pH 6.8, 70 mM NaCl, and the cytosol of the cells also contained ~5 mM of a reducing agent (glutathione) (45). Therefore, we can state that a stable and tight interaction between p75NTR DDs in a C257 disulfide-linked dimer is rather unlikely under reducing conditions, although transient and weak interactions are still possible.

Taken together, our observations indicate that the snail-tong model fits the in vivo data well, but contradicts the structural information; therefore, we have to consider other possible mechanisms of p75NTR activation. The first and most obvious possibility is ligand-induced dimerization (Fig. 5 *B*). The formation of the C257 covalent dimer has been reported to be concentration dependent (10); thus, at normal expression levels, the fraction of disulfide-linked dimers on the cell surface may be negligible, and at such levels the dimerization could be triggered mainly by ligand

binding. On the other hand, it was shown that although PC12 cells express p75 and no NGF, they still demonstrate significant levels of p75 covalent dimers, as do hippocampal and cortical neurons (10). Therefore, ligand-induced dimerization must not be considered as a prospective candidate for the p75NTR activation mechanism. Thus, we need to search for a process, with both ligand-bound and ligand-free states of the receptor being disulfide-linked dimers, and with no direct relationship between the structures of the TMD and ICD and the process, that does not require a tight interaction between the DDs in the inactive state.

The first option is that ligand binding causes a transfer of the receptor toward a certain compartment of the membrane (e.g., lipid rafts), and it is activated by clustering, as is the case with other TNFR family members. In this model, Cys-257 would facilitate the clustering process. Another possibility is that the binding of the NGF to the preformed dimers induces a conformational change close to the TMD that induces internalization of the receptor or shedding of p75 and intracellular signaling after γ-secretase cleavage (Fig. 5). The latter two mechanisms do not contradict either the data reported by Vilar et al. (10) or the structural and dynamic parameters of the p75NTR-based constructs obtained in this work, because the information on ligand binding does not need to be transferred to the cytoplasmic domains or affect their structure. These two scenarios need to be tested in the future by functional assays to confirm or disprove our speculations.

Our data suggest that the ICD of p75NTR has no rigidity, which is necessary to undergo a conformational change upon ligand binding. However, our work was performed in vitro without the ligand or the NGF binding domain, and in the absence of cellular factors. Different lipids in the plasma membrane or posttranslational modifications also need to be taken into account. Therefore, the snail-tong model should not be completely dismissed, especially since we were not able to assemble the C257 S-S linked dimer of p75-ΔECD. The chopper domain may be constitutively bound to intracellular factors in the absence of ligand that make it rigid and able to transmit the force generated by ligand binding. Or the chopper domain may become structured in the covalent dimers of p75NTR and therefore able to change its conformation and transfer the information about the state of the TMD in response to ligand binding. Assembly of the C257 disulfide-bound dimer of p75-ΔECD is necessary to resolve this problem, and will be the subject of our future research.

CONCLUSIONS

In summary, we have described the structural properties and intramolecular mobilities of the chopper domain and DDs in the presence of the TMD of p75NTR in a near-native environment provided by LPNs, and in detergent micelles/lipid bicelles. We have shown that such nanodiscs are applicable for structural studies of membrane proteins containing large soluble domains, and demonstrated that the data obtained in LPNs may provide insights into the molecular mechanisms of essential biological processes.

SUPPORTING MATERIAL

Supporting Materials and Methods and nine figures are available at http://www.biophysj.org/biophysj/supplemental/S0006-3495(15)00714-6.

AUTHOR CONTRIBUTIONS

K.S.M. performed the NMR experiments, analyzed the data, and wrote the article. S.A.G. assembled LPNs, expressed the proteins, analyzed the data, and contributed to the writing of the article. P.K.K. performed the light-scattering experiments and MSP expression and purification. M.V. performed in silico prediction and contributed to the writing of the article. A.S.A. supervised the project.

ACKNOWLEDGMENTS

We thank the group of Prof. G. Wagner (Harvard Medical School) and E. Lyukmanova (IBCh RAS) for kindly providing the plasmids for MSP expression.

This work was supported by the Russian Science Foundation (project 14-50-00131, MSP production and LPN assembly protocols), the Russian Foundation for Basic Research (project 13-04-40107-H, protein expression and NMR experiments), and the Spanish Ministry of Competitiveness (MINECO, BFU-42746-P to M.V.).

SUPPORTING CITATIONS

References (46,47) appear in the Supporting Material.

REFERENCES

1. Ibáñez, C. F., and A. Simi. 2012. p75 neurotrophin receptor signaling in nervous system injury and degeneration: paradox and opportunity. *Trends Neurosci.* 35:431–440.
2. Hu, Y., X. Lee, …, S. Mi. 2013. A DR6/p75(NTR) complex is responsible for β-amyloid-induced cortical neuron death. *Cell Death Dis.* 4:e579.
3. Knowles, J. K., D. A. Simmons, …, F. M. Longo. 2013. Small molecule p75NTR ligand prevents cognitive deficits and neurite degeneration in an Alzheimer's mouse model. *Neurobiol. Aging.* 34:2052–2063.
4. Longo, F. M., and S. M. Massa. 2013. Small-molecule modulation of neurotrophin receptors: a strategy for the treatment of neurological disease. *Nat. Rev. Drug Discov.* 12:507–525.
5. Longo, F. M., and S. M. Massa. 2008. Small molecule modulation of p75 neurotrophin receptor functions. *CNS Neurol. Disord. Drug Targets.* 7:63–70.
6. Ovsepian, S. V., and J. Herms. 2013. Drain of the brain: low-affinity p75 neurotrophin receptor affords a molecular sink for clearance of cortical amyloid β by the cholinergic modulator system. *Neurobiol. Aging.* 34:2517–2524.
7. Kraemer, B. R., S. O. Yoon, and B. D. Carter. 2014. The biological functions and signaling mechanisms of the p75 neurotrophin receptor. *Handbook Exp. Pharmacol.* 220:121–164.
8. Gentry, J. J., P. A. Barker, and B. D. Carter. 2004. The p75 neurotrophin receptor: multiple interactors and numerous functions. *Prog. Brain Res.* 146:25–39.

9. Coulson, E. J., K. Reid, …, P. F. Bartlett. 2000. Chopper, a new death domain of the p75 neurotrophin receptor that mediates rapid neuronal cell death. *J. Biol. Chem.* 275:30537–30545.
10. Vilar, M., I. Charalampopoulos, …, C. F. Ibáñez. 2009. Activation of the p75 neurotrophin receptor through conformational rearrangement of disulphide-linked receptor dimers. *Neuron.* 62:72–83.
11. Vilar, M., T.-C. Sung, …, K.-F. Lee. 2014. Heterodimerization of p45-p75 modulates p75 signaling: structural basis and mechanism of action. *PLoS Biol.* 12:e1001918.
12. Qu, Q., J. Chen, …, T. Jiang. 2013. Structural characterization of the self-association of the death domain of p75(NTR). *PLoS One.* 8:e57839.
13. Liepinsh, E., L. L. Ilag, …, C. F. Ibáñez. 1997. NMR structure of the death domain of the p75 neurotrophin receptor. *EMBO J.* 16:4999–5005.
14. Spirin, A. S., V. I. Baranov, …, Y. B. Alakhov. 1988. A continuous cell-free translation system capable of producing polypeptides in high yield. *Science.* 242:1162–1164.
15. Schwarz, D., F. Junge, …, F. Bernhard. 2007. Preparative scale expression of membrane proteins in Escherichia coli-based continuous exchange cell-free systems. *Nat. Protoc.* 2:2945–2957.
16. Kai, L., C. Roos, …, F. Bernhard. 2012. Systems for the cell-free synthesis of proteins. *Methods Mol. Biol.* 800:201–225.
17. Goncharuk, S. A., M. V. Goncharuk, …, M. P. Kirpichnikov. 2011. Bacterial synthesis and purification of normal and mutant forms of human FGFR3 transmembrane segment. *Acta Naturae.* 3:77–84.
18. Studier, F. W. 2005. Protein production by auto-induction in high density shaking cultures. *Protein Expr. Purif.* 41:207–234.
19. Ritchie, T. K., Y. V. Grinkova, …, S. G. Sligar. 2009. Chapter 11—Reconstitution of membrane proteins in phospholipid bilayer nanodiscs. *Methods Enzymol.* 464:211–231.
20. Cavanagh, J., W. J. Fairbrother, …, N. J. Skelton. 2007. Protein NMR Spectroscopy: Principles and Practice, 2nd ed. Academic Press, Burlington, MA.
21. Orekhov, V. Y., and V. A. Jaravine. 2011. Analysis of non-uniformly sampled spectra with multi-dimensional decomposition. *Prog. Nucl. Magn. Reson. Spectrosc.* 59:271–292.
22. Favier, A., and B. Brutscher. 2011. Recovering lost magnetization: polarization enhancement in biomolecular NMR. *J. Biomol. NMR.* 49:9–15.
23. Farrow, N. A., R. Muhandiram, …, L. E. Kay. 1994. Backbone dynamics of a free and phosphopeptide-complexed Src homology 2 domain studied by 15N NMR relaxation. *Biochemistry.* 33:5984–6003.
24. Chill, J. H., J. M. Louis, …, A. Bax. 2006. Measurement of 15N relaxation in the detergent-solubilized tetrameric KcsA potassium channel. *J. Biomol. NMR.* 36:123–136.
25. Sørland, G. H., D. Aksnes, and L. Gjerdåker. 1999. A pulsed field gradient spin-echo method for diffusion measurements in the presence of internal gradients. *J. Magn. Reson.* 137:397–401.
26. Shen, Y., F. Delaglio, …, A. Bax. 2009. TALOS+: a hybrid method for predicting protein backbone torsion angles from NMR chemical shifts. *J. Biomol. NMR.* 44:213–223.
27. Underwood, C. K., K. Reid, …, E. J. Coulson. 2008. Palmitoylation of the C-terminal fragment of p75(NTR) regulates death signaling and is required for subsequent cleavage by gamma-secretase. *Mol. Cell. Neurosci.* 37:346–358.
28. Shenkarev, Z. O., E. N. Lyukmanova, …, A. S. Arseniev. 2010. Lipid-protein nanodiscs as reference medium in detergent screening for high-resolution NMR studies of integral membrane proteins. *J. Am. Chem. Soc.* 132:5628–5629.
29. Tzitzilonis, C., C. Eichmann, …, R. Riek. 2013. Detergent/nanodisc screening for high-resolution NMR studies of an integral membrane protein containing a cytoplasmic domain. *PLoS One.* 8:e54378.
30. Bayburt, T. H., and S. G. Sligar. 2010. Membrane protein assembly into nanodiscs. *FEBS Lett.* 584:1721–1727.
31. Hagn, F., M. Etzkorn, …, G. Wagner. 2013. Optimized phospholipid bilayer nanodiscs facilitate high-resolution structure determination of membrane proteins. *J. Am. Chem. Soc.* 135:1919–1925.
32. Shenkarev, Z. O., E. N. Lyukmanova, …, A. S. Arseniev. 2013. Lipid-protein nanodiscs promote in vitro folding of transmembrane domains of multi-helical and multimeric membrane proteins. *Biochim. Biophys. Acta.* 1828:776–784.
33. Lyukmanova, E. N., Z. O. Shenkarev, …, A. S. Arseniev. 2008. Lipid-protein nanoscale bilayers: a versatile medium for NMR investigations of membrane proteins and membrane-active peptides. *J. Am. Chem. Soc.* 130:2140–2141.
34. Shenkarev, Z. O., E. N. Lyukmanova, …, A. S. Arseniev. 2009. Lipid-protein nanodiscs: possible application in high-resolution NMR investigations of membrane proteins and membrane-active peptides. *Biochemistry (Mosc.).* 74:756–765.
35. Shenkarev, Z. O., E. N. Lyukmanova, …, A. S. Arseniev. 2014. Lipid-protein nanodiscs offer new perspectives for structural and functional studies of water-soluble membrane-active peptides. *Acta Naturae.* 6:84–94.
36. Shenkarev, Z. O., A. S. Paramonov, …, A. S. Arseniev. 2013. Peptaibol antiamoebin I: spatial structure, backbone dynamics, interaction with bicelles and lipid-protein nanodiscs, and pore formation in context of barrel-stave model. *Chem. Biodivers.* 10:838–863.
37. Hagn, F., and G. Wagner. 2015. Structure refinement and membrane positioning of selectively labeled OmpX in phospholipid nanodiscs. *J. Biomol. NMR.* 61:249–260.
38. Tugarinov, V., and L. E. Kay. 2003. Ile, Leu, and Val methyl assignments of the 723-residue malate synthase G using a new labeling strategy and novel NMR methods. *J. Am. Chem. Soc.* 125:13868–13878.
39. Muona, M., A. S. Aranko, and H. Iwai. 2008. Segmental isotopic labelling of a multidomain protein by protein ligation by protein trans-splicing. *ChemBioChem.* 9:2958–2961.
40. Vilar, M., I. Charalampopoulos, …, C. F. Ibáñez. 2009. Ligand-independent signaling by disulfide-crosslinked dimers of the p75 neurotrophin receptor. *J. Cell Sci.* 122:3351–3357.
41. Khursigara, G., J. R. Orlinick, and M. V. Chao. 1999. Association of the p75 neurotrophin receptor with TRAF6. *J. Biol. Chem.* 274:2597–2600.
42. Mukai, J., T. Hachiya, …, T. A. Sato. 2000. NADE, a p75NTR-associated cell death executor, is involved in signal transduction mediated by the common neurotrophin receptor p75NTR. *J. Biol. Chem.* 275:17566–17570.
43. Casademunt, E., B. D. Carter, …, Y. A. Barde. 1999. The zinc finger protein NRIF interacts with the neurotrophin receptor p75(NTR) and participates in programmed cell death. *EMBO J.* 18:6050–6061.
44. Coulson, E. J., K. Reid, …, P. F. Bartlett. 2004. The role of neurotransmission and the Chopper domain in p75 neurotrophin receptor death signaling. *Prog. Brain Res.* 146:41–62.
45. Appenzeller-Herzog, C. 2011. Glutathione- and non-glutathione-based oxidant control in the endoplasmic reticulum. *J. Cell Sci.* 124:847–855.
46. Dosztányi, Z., V. Csizmok, …, I. Simon. 2005. IUPred: web server for the prediction of intrinsically unstructured regions of proteins based on estimated energy content. *Bioinformatics.* 21:3433–3434.
47. Schägger, H., and G. von Jagow. 1987. Tricine-sodium dodecyl sulfate-polyacrylamide gel electrophoresis for the separation of proteins in the range from 1 to 100 kDa. *Anal. Biochem.* 166:368–379.